JOINT DRIVER INTENTION CLASSIFICATION AND TRACKING OF VEHICLES

*J. Gunnarsson, L. Svensson**

Chalmers University of Technology
Department of Signals and Systems
Göteborg, Sweden
joakim.gunnarsson@s2.chalmers.se
lennart.svensson@chalmers.se

F. Bengtsson†, L. Danielsson††

Volvo 3P†
Volvo Car Corporation††
Göteborg, Sweden
fredrik.bengtsson@volvo.com
ldanie25@volvocars.com

ABSTRACT

In this paper we present and validate a new modelling framework for joint driver intention classification and tracking of vehicles; a framework derived for automotive active safety systems. Such systems require reliable predictions of the traffic situation to act in time when a dangerous situation occur. Our proposal has two main benefits. First, it incorporates the intention of the driver into the vehicle motion model and thereby improves the prediction capability. The result is a multiple motion model where each model corresponds to a specific driver intent. Second, the connection between different driver plans and corresponding motion model enables a formal classification of the most likely driver intention. To validate our concept, we apply the motion model on real data using a particle filter implementation. Initial studies indicate promising performance.

1. INTRODUCTION

A current trend in today's automotive industry, is to equip vehicles with active safety systems. These have the objective to aid the driver in different accident prone situations *e.g.* unintentional lane departures, or dangers caused by distracted drivers. Based on sensor information, active safety systems try to assess the situation and detect dangerous scenarios. This task requires the system to track the environment surrounding the vehicle.

In this paper we suggest a model for joint tracking and driver intention classification. Such a scheme is enabled by pre-defining a set of possible driver intentions such as *lane change maneuvers*, *overtaking maneuvers*, and *lane following*. Additionally, by representing the different driver modes with a discrete parameter and constructing situation specific motion models, we can jointly track the vehicle and select the most likely driver mode. By performing the tracking and driver intention classification simultaneously, we expect an improved performance for both tasks.

The proposed algorithm requires situation specific motion models, and in this paper we extend the model presented in [1]. Instead of only handling a single motion model where the driver intends to follow the lane, we now include lane change maneuvers as an alternative driver mode. The result is a multiple motion model with which we can evaluate our situation specific motion models, and examine if they can be used for joint driver intention classification and object tracking.

2. PROBLEM FORMULATION

In tracking, we seek to calculate the posterior density function (pdf) $p(\mathbf{x}(k)|\mathbf{Y}(k))$ for the state vector $\mathbf{x}(k)$. Using $p(\mathbf{x}(k)|\mathbf{Y}(k))$, we can compute estimates and uncertainty measures of our quantities of interest in $\mathbf{x}(k)$. The estimates are based on all available measurements $\mathbf{Y}(k) \triangleq \{\mathbf{y}(i),\ i = 1,\dots,k\}$, where $\mathbf{y}(k)$ is a vector of measurements collected at time k. The discrete time index k is assigned to a continuous time instant, t_k, and the update interval is denoted $T_s \triangleq t_k - t_{k-1}$. The state vector is assumed to evolve with time according to the process model

$$\mathbf{x}(k+1) = f_k(\mathbf{x}(k), \mathbf{w}(k)), \tag{1}$$

and the measurements are assumed to be related to the state vector according to the measurement model

$$\mathbf{y}(k) = h_k(\mathbf{x}(k), \mathbf{v}(k)). \tag{2}$$

In (1), $\mathbf{w}(k)$ is a noise process included to reflect model uncertainties and $\mathbf{v}(k)$ in (2) is a measurement noise process capturing both model uncertainties and measurement disturbances. Both $\mathbf{w}(k)$ and $\mathbf{v}(k)$ are assumed to be zero-mean Gaussian distributed with known covariance matrices $\mathbf{Q}(k)$ and $\mathbf{R}(k)$ respectively.

In this article we limit the tracking problem by only considering two-lane roads and single vehicle scenarios. To describe the vehicle's position and motion, we use different coordinate systems described in Fig. 1. First of all, we employ a

*This work was sponsored by the Swedish Intelligent Vehicle Safety Systems (IVSS) program, and is a part of the SEnsor Fusion for Safety Systems (SEFS) project.

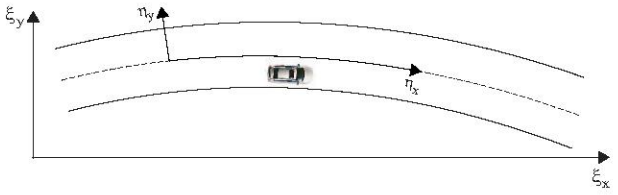

Fig. 1: This figure illustrates the global Cartesian coordinate system, and the curved road coordinate system.

curved *road coordinate system* (η_x, η_y), previously been used in *e.g.* [2]. For most of our calculations, the motion of the vehicle is conveniently described by the vector

$$\mathbf{z}(k) = [\eta_x(k)\ \eta_y(k)\ \dot{\eta}_x(k)\ \dot{\eta}_y(k)\ \ddot{\eta}_x(k)\ \ddot{\eta}_y(k)]^T, \quad (3)$$

where $\dot{\eta}(k)$ and $\ddot{\eta}(k)$ are the first and second time derivatives, respectively. Second, the motion model we propose requires a global Cartesian coordinate system (ξ_x, ξ_y). The use of the (ξ_x, ξ_y) coordinate system is motivated further in 3.4.3.

Apart from tracking the physical quantities in $\mathbf{z}(k)$, we wish to estimate the intention of the driver, represented by a discrete model parameter $M(k)$. In this study $M(k) \in \{1, 2, 3, 4\}$, and the interpretation of these four hypotheses are

$$M(k) = 1: \quad \text{vehicle follows the right lane} \quad (4)$$
$$M(k) = 2: \quad \text{vehicle follows the left lane} \quad (5)$$
$$M(k) = 3: \quad \text{vehicle changes to the right lane} \quad (6)$$
$$M(k) = 4: \quad \text{vehicle changes to the left lane.} \quad (7)$$

To interpret the estimates of $\mathbf{z}(k)$ expressed in the road coordinate system, we also need a model of the road. In this article, we follow suggestions from e.g. [3] and use a clothoid model to define the road. According to this model the curvature of the road changes as a linear function,

$$c(\eta_x) = c_0 + \eta_x c_1. \quad (8)$$

The clothoid parameters $c_0(k)$, $c_1(k)$ and the lane width $LW(k)$ are stored in a separate road state vector $\mathbf{r}(k) = [LW(k)\ c_0(k)\ c_1(k)]^T$. This vector is unknown and together with $\mathbf{z}(k)$ and $M(k)$ make up the complete state vector

$$\mathbf{x}(k) = \left[\mathbf{r}(k)^T\ \mathbf{z}(k)^T\ M(k)\right]^T. \quad (9)$$

3. PROCESS MODEL

The process model defined in (1) describes how the state vector $\mathbf{x}(k)$ evolves in one time step T_s. We will divide this model into three separate models: one for the road state vector $\mathbf{r}(k)$, one for the driver intention parameter $M(k)$, and one for the vehicle motion state vector $\mathbf{z}(k)$. Similarly, we split the process noise, $\mathbf{w}(k)$, into three mutually independent parts

$$\mathbf{w}(k) = [\mathbf{w}_r(k)\ w_M(k)\ \mathbf{w}_z(k)]^T. \quad (10)$$

Each of the three process models are presented in the remainder of this section.

3.1. Modelling road parameters

To describe the evolution of $\mathbf{r}(k)$, we use the model

$$\mathbf{r}(k+1) = \begin{bmatrix} 1 & 0 & 0 \\ 0 & 1 & T_s\dot{\eta}_x(k) \\ 0 & 0 & 1 \end{bmatrix} \mathbf{r}(k) + \mathbf{w}_\mathbf{r}(k), \quad (11)$$

proposed *e.g.* in [2]. Here, $\mathbf{w}_r(k)$ is a white Gaussian noise vector with covariance matrix $\mathbf{Q}_\mathbf{r}(k)$.

3.2. Modelling changes in driver intentions

The driver intentions reflected by the discrete model parameter $M(k)$ controls which of the intention specific motion models for $\mathbf{z}(k)$ is in use during the time interval $(t_{k-1}, t_k]$. The process noise $w_M(k)$ is such that $M(k)$ is a first order Markov chain. The transitional probabilities are defined as

$$\pi_{ij}(k+1) \triangleq \Pr\{M(k+1) = j | M(k) = i, \mathbf{x}(k)\}, \quad (12)$$

where $i, j \in [1, 2, 3, 4]$, $\pi_{ij}(k) > 0$, and $\sum_{j=1}^{4} \pi_{ij}(k) = 1$.

When more vehicles are included in the model, the transitional probabilities will also depend on the state of those vehicles.

3.3. Modelling vehicle motion

As previously mentioned, we propose a multiple motion model for $\mathbf{z}(k)$, where the different models depend on the intention of the driver, given by $M(k)$. To describe the motion of the vehicle, we use the modified constant acceleration (CA) model structure presented in [1]

$$\mathbf{z}(k+1) = \mathbf{A}\mathbf{z}(k) + \mathbf{B}\mathbf{u}(k) + \mathbf{B}\mathbf{w}_\mathbf{z}(k), \quad (13)$$

where $\mathbf{w}_\mathbf{z}(k) \sim \mathcal{N}(0, \mathbf{Q}_\mathbf{z}(k))$ and

$$\mathbf{A} = \begin{bmatrix} 1 & 0 & T_s & 0 & T_s^2/2 & 0 \\ 0 & 1 & 0 & T_s & 0 & T_s^2/2 \\ 0 & 0 & 1 & 0 & T_s & 0 \\ 0 & 0 & 0 & 1 & 0 & T_s \\ 0 & 0 & 0 & 0 & 1 & 0 \\ 0 & 0 & 0 & 0 & 0 & 1 \end{bmatrix}, \quad (14)$$

$$\mathbf{B} = \begin{bmatrix} T_s^2/6 & 0 \\ 0 & T_s^2/6 \\ T_s/2 & 0 \\ 0 & T_s/2 \\ 1 & 0 \\ 0 & 1 \end{bmatrix}, \quad \mathbf{u}(k) = \begin{bmatrix} a_{\eta_x}(k) \\ a_{\eta_y}(k) \end{bmatrix}. \quad (15)$$

The scalar functions $a_{\eta_x}(k)$ and $a_{\eta_y}(k)$ are approximations of the accelerations imposed by the driver, and we use accelerations from an *optimal vehicle state trajectory* as $a_{\eta_x}(k)$

and $a_{\eta_y}(k)$. The trajectory depends, of course, on the driver intention $M(k)$, and this is also how $\mathbf{z}(k+1)$ depends on $M(k+1)$. We limit the set of trajectories to those whose accelerations change linearly between the sample instances. This restriction explains the form of $\mathbf{B}$ in (15), and more importantly gives that the optimal vehicle state trajectory, $\mathbf{z}(k+1)\ \ldots\ \mathbf{z}(k+N)$, is completely described by the initial state, $\mathbf{x}(k)$, and the matrix of triple derivatives, jerks,

$$\mathbf{j}(k) = \begin{bmatrix} \dddot{\eta}_x(k) & \dddot{\eta}_x(k+1) & \ldots & \dddot{\eta}_x(k+N-1) \\ \dddot{\eta}_y(k) & \dddot{\eta}_y(k+1) & \ldots & \dddot{\eta}_y(k+N-1) \end{bmatrix}. \tag{16}$$

The optimal sequence of triple derivatives, $\mathbf{j}(k)$, is found by minimizing the cost function

$$\underset{\mathbf{j}(k)}{\text{minimize}} \quad \sum_{l=k}^{k+N-1} \text{cost}(\mathbf{r}(k), M(k), \mathbf{z}(l), \dddot{\eta}_x(l), \dddot{\eta}_y(l)). \tag{17}$$

The cost function in (17) is based on that in [1], and is constructed to capture different aspects, considered by the driver, when planning the route ahead.

3.4. Cost Functions

By only considering single vehicle scenarios, the cost function can be divided into three components: the longitudinal velocity, $c_{lo}(\dot{\eta}_x(l), M(k))$, the lateral positioning of the vehicle, $c_{la}(\eta_y(l), M(k))$, and the comfort of the predicted trajectory, $c_c(\dddot{\eta}_x(l), \dddot{\eta}_y(l), \mathbf{z}(l)$. A weighted sum of the different components constitutes the total cost

$$\begin{aligned} &\text{cost}(\mathbf{r}(k), M(k), \mathbf{z}(l), \dddot{\eta}_x(l), \dddot{\eta}_y(l)) = \alpha_{lo} c_{lo}(\dot{\eta}_x(l), M(k)) \\ &+ \alpha_{la} c_{la}(\eta_y(l), M(k)) + \alpha_c c_c(\dddot{\eta}_x(l), \dddot{\eta}_y(l), \mathbf{z}(l)), \end{aligned} \tag{18}$$

where the parameters $\alpha_{lo}, \alpha_{la}, \alpha_c$, decide how the driver give priority to the different cost functions.

3.4.1. *Longitudinal cost function, $c_{lo}(\dot{\eta}_x(l), M(k))$*

In [1], two separate cost functions were defined to describe the longitudinal velocity. Here, we combine these into one cost function, which due to the single vehicle scenario is independent of the driver intention parameter

$$c_{lo}(\dot{\eta}_x(l), M(k)) = (\dot{\eta}_x(l) - \dot{\eta}_{\text{x-ref}})^2. \tag{19}$$

The reference velocity $\dot{\eta}_{\text{x-ref}}$ is an important model parameter describing which velocity the driver aims at keeping.

3.4.2. *Lateral cost function, $c_{la}(\eta_y(l), M(k))$*

The lateral cost depends on the driver intention and the lateral position of the vehicle. If the intention is to follow the lane, large costs will be associated with trajectories outside the lane. For the lane change hypothesis the cost is set as

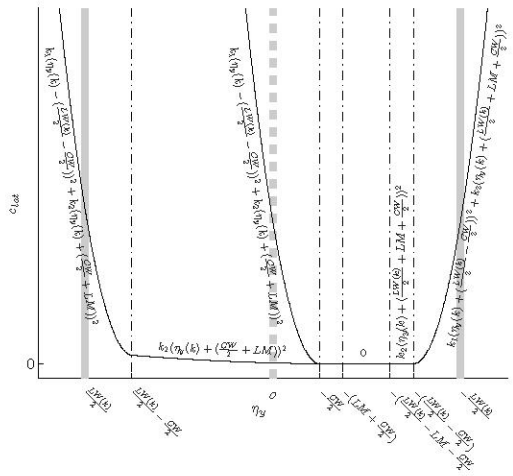

Fig. 2: Lateral cost functions for following the right lane and changing lane from left to right. In the figure the mathematical expressions for the different road region are specified.

to, in conjunction with $c_c(\dddot{\eta}_x(l), \dddot{\eta}_y(l), \mathbf{z}(l))$, encourage a smooth transition from one lane to the other. In Fig. 2, the lateral cost is plotted for $M(k) \in \{1, 3\}$. The background consists of a road, portrayed with thick grey lines divided into different cost segments. In the expressions CW is the width of car and LM is a margin to the lane edge, whereas k_1 and k_2 are design parameters used to tune the cost functions. For $M(k) \in \{2, 4\}$ an analogue approach is used.

3.4.3. *The comfort cost function $c_c(\dddot{\eta}_x(l), \dddot{\eta}_y(l), \mathbf{z}(l))$*

This cost function corresponds to the driver's desire to steer the vehicle in a smooth and comfortable manner. Smooth trajectories are accomplished by increasing the cost for large accelerations and jerks. However, the acceleration perceived by the driver is not equal to the acceleration of the vehicle expressed in curved road coordinates. Instead the global Cartesian coordinate system (ξ_x, ξ_y), is used. It is easy to construct a mapping $T : \mathbb{R}^2 \to \mathbb{R}^2$ from road coordinates to Cartesian coordinates, i.e., T is such that $T(\eta_x, \eta_y) = [\xi_x\ \xi_y]^T$. Using the mapping T it is also possible to compute $(\ddot{\xi}_x(l), \ddot{\xi}_y(l))$ and $(\dddot{\xi}_x(l), \dddot{\xi}_y(l))$ from $\mathbf{z}(l)$, and $(\dddot{\eta}_x(l), \dddot{\eta}_y(l))$.

Additionally, to simplify the expressions we introduce the notation $\ddot{\xi}(l) = \sqrt{\ddot{\xi}_x(l)^2 + \ddot{\xi}_y(l)^2}$ and $\dddot{\xi}(l) = \sqrt{\dddot{\xi}_x(l)^2 + \dddot{\xi}_y(l)^2}$. The cost function is divided into two parts: one which is related to the acceleration, c_{a}, and one which is relate to the jerk, c_{j}. We write the cost function as

$$c_{\text{c}}(\dddot{\eta}_x(l), \dddot{\eta}_y(l), \mathbf{z}(l)) = c_{\text{a}}(\ddot{\xi}(l)) + c_{\text{j}}(\dddot{\xi}(l)). \tag{20}$$

In [1] we used information from [4] to set limits on the acceleration and jerk for normal and uncomfortable driving. Here

we have used the same limits and a similar cost function

$$c_a(\ddot{\xi}(k)) = \begin{cases} \left(\frac{\ddot{\xi}(k)}{0.5}\right)^2 & \text{if } \ddot{\xi}(k) < 0.5 \\ \left(\frac{5}{6} + \frac{2\ddot{\xi}(k)^6}{0.5^5 6}\right)^2 & \text{if } \ddot{\xi}(k) \geq 0.5 \end{cases} \quad (21)$$

$$c_j(\dddot{\xi}(k)) = \begin{cases} \left(\frac{\dddot{\xi}(k)}{1.5}\right)^2 & \text{if } \dddot{\xi}(k) < 1.5 \\ \left(-\frac{1}{2} + \frac{2\dddot{\xi}(k)^2}{3}\right)^2 & \text{if } \dddot{\xi}(k) \geq 1.5. \end{cases} \quad (22)$$

4. NUMERICAL EXAMPLE

To evaluate the proposed model, we use data from a forward looking vision sensor and a set of internal vehicle sensors. The vision sensor provides information about the curvature of the road, $c_0^m(k)$, as well as the vehicle's lateral distance to the left lane markings, $L^m(k)$, and right lane markings, $R^m(k)$. From the internal sensors we collect quantities such as speed $v^m(k)$, magnitude of the acceleration, $a^m(k)$, heading angle, $\psi(k)$, and yaw rate, $\dot{\psi}_{\text{abs}}(k)$. The measurements are stored in the measurement vector

$$\mathbf{y}(k) = [c_0^m(k)\ v^m(k)\ a^m(k)\ \psi(k)\ \dot{\psi}_{\text{abs}}(k)\ L^m(k)\ R^m(k)]^T, \quad (23)$$

and a relation to the state vector $\mathbf{x}(k)$ is found using the following measurement model

$$c_0^m(k) = c_0(k) + v_1(k) \quad (24)$$

$$v^m(k) = \sqrt{\dot{\eta}_x(k)^2 + \dot{\eta}_y(k)^2} + v_2(k) \quad (25)$$

$$a^m(k) = \sqrt{\ddot{\eta}_x(k)^2 + \ddot{\eta}_y(k)^2} + v_3(k) \quad (26)$$

$$\psi(k) = \arctan\left(\frac{\dot{\eta}_y(k)}{\dot{\eta}_x(k)}\right) + v_4(k) \quad (27)$$

$$\dot{\psi}_{\text{abs}}(k) = \frac{\dot{\eta}_x(k)\ddot{\eta}_y(k) - \dot{\eta}_y(k)\ddot{\eta}_x(k)}{\dot{\eta}_x(k)^2 + \dot{\eta}_y(k)^2} \quad (28)$$

$$- c_0(k)\sqrt{\dot{\eta}_x(k)^2 + \dot{\eta}_y(k)^2} + v_5(k). \quad (29)$$

The models for the lane distances are different depending on which lane the vehicle is positioned in. When the vehicle is positioned in the right lane ($\eta_y < 0$) the model takes the form

$$L^m(k) = \eta_y(k) + v_6(k) \quad (30)$$

$$R^m(k) = LW(k) + \eta_y(k) + v_7(k). \quad (31)$$

The suggested models ability to detect lane change maneuvers is tested using a 29 seconds long data sequence involving two lane change maneuvers. A particle filter with 5000 particles is used to estimate the posterior pdf of $\mathbf{x}(k)$. The model uncertainties are set to $\mathbf{Q}_x(k) = \text{diag}[0.47\ 0.47]$, and $\mathbf{Q}_r(k) = 1.5 \cdot 10^{-4}\text{diag}[1\ 10\ 1]$, $\mathbf{R}(k) = \text{diag}[2 \cdot 10^{-6}\ 0.24\ 1\ 0.1\ 0.015\ 0.1\ 0.1]$. Moreover, the transitional probabilities in (12) are set to zero except for $\eta_y(k-1) > 0$: $\pi_{22}(k) = 0.73$, $\pi_{23}(k) = 0.27$, and $\eta_y(k-1) < 0$: $\pi_{11}(k) = 0.73$, $\pi_{14}(k) = 0.27$. The following values of the α parameters in (18) are used: $\alpha_{lo} = 1$, $\alpha_{la} = 0.7$, and $\alpha_c = 5$. The reference velocity is held constant to $\dot{\eta}_{x-ref} = 34$ m/s.

Fig. 3 presents the estimated lateral position of the vehicle during two lane change maneuvers. Additionally, the probabilities of lane change maneuvers are also plotted. As can be seen, the suggested algorithm is able to predict the lane change maneuvers before the vehicle crosses the lane markings.

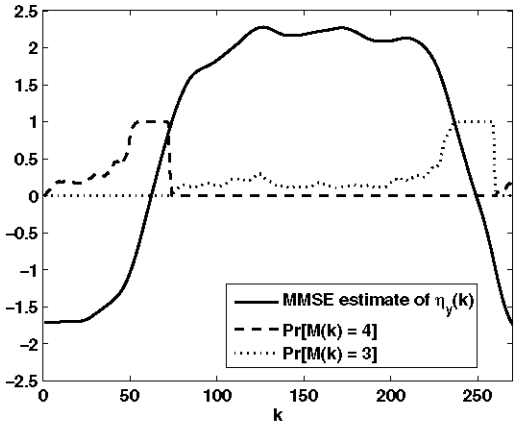

Fig. 3: The solid curve represents the MMSE estimate of the lateral position of the vehicle. The dashed line is the probability of a lane change to the left, and the dotted curve is the probability of a lane change to the right.

5. REFERENCES

[1] L. Svensson and J. Gunnarsson, "A new motion model for tracking of vehicles," in *14th IFAC Symposium on System Identification*, Newcastle, Australia, March 2006.

[2] Andreas Eidehall, "An automotive lane guidance system," Tech. Rep. Licentiate Thesis no. 1122, Department of Electrical Engineering, Linkping University, SE-581 83 Linkping, Sweden, Nov 2004.

[3] E.D. Dickmanns and A. Zapp, "A curvature-based scheme for improving road vehicle guidance by computer vision," in *Proceedings of the SPIE Conference on Mobile Robots*, 1986.

[4] "Vgu, vv publikation 2004:80, grundvärden," June 2004, ISSN: 1401-9612.